Cell Tissue Res (2003) 312:155–165
DOI 10.1007/s00441-003-0713-5

REGULAR ARTICLE

Michael Becker · Hans Gerd Nothwang · Eckhard Friauf

Differential expression pattern of chloride transporters *NCC, NKCC2, KCC1, KCC3, KCC4,* and *AE3* in the developing rat auditory brainstem

Received: 30 August 2002 / Accepted: 19 February 2003 / Published online: 24 April 2003

Abstract During development of inhibitory synapses, the action of the two neurotransmitters GABA and glycine shifts from depolarizing to hyperpolarizing. The shift is due to an age-dependent regulation of the intracellular free chloride concentration ($[Cl^-]_i$) in postsynaptic neurons. A model system to study this maturation process is a glycinergic projection in the mammalian auditory brainstem. It is formed in the superior olivary complex (SOC) by neurons of the medial nucleus of the trapezoid body, whose axons terminate in the lateral superior olive (LSO). LSO neurons of perinatal rats and mice are depolarized upon glycine application, whereas older cells (>postnatal day (P) 8) are hyperpolarized. Here we examined the expression of six secondary active chloride transporter genes (*NCC, NKCC2, KCC1, KCC3, KCC4,* and *AE3*) in the rat SOC to unravel the molecular mechanisms underlying this change. RT-PCR analysis demonstrated brainstem expression of *KCC1, KCC3, KCC4,* and *AE3*, but not of *NCC* and *NKCC2*. RNA in situ hybridization showed that only *AE3* is highly expressed both at P3 (high $[Cl^-]_i$) and P12 (low $[Cl^-]_i$) in LSO neurons. *KCC1* and *KCC4* are weakly expressed in LSO neurons at P3 and P12, respectively. This study completes the expression analysis of all known chloride transporters sensitive to loop diuretic drugs in the SOC and demonstrates differences in the maturation between hippocampal and brainstem inhibitory synapses.

This work was supported by the Deutsche Forschungsgemeinschaft (SFB 530 grant to E.F.)

M. Becker · H. G. Nothwang · E. Friauf
Abteilung Tierphysiologie, Universität Kaiserslautern, Kaiserslautern, Germany

E. Friauf (✉)
Abteilung Tierphysiologie,
Fachbereich Biologie, Universität Kaiserslautern,
Postfach 3049, 67653 Kaiserslautern, Germany
e-mail: friauf@rhrk.uni-kl.de
Tel.: +49-631-2052424
Fax: +49-631-2054684

Keywords In situ hybridization · Brain development · Inhibitory synapses · Superior olivary complex · Rat (Sprague Dawley)

Introduction

Inhibitory synapses constitute about 30% of all synapses in the central nervous system (CNS) and are essential for the proper function of neural circuits. They are involved in several aspects of neuronal information processing, they regulate oscillatory behavior of neuronal networks, and they prevent the spread of excitatory activity; their failure can lead to pathological conditions such as epilepsy (reviews: Alvarez-Leefmans 1990; Mehta and Ticku 1999; Delpire 2000; Legendre 2001). For a better understanding of normal and pathological brain function, it is essential to identify the molecular mechanisms underlying inhibitory neurotransmission and the ontogenetic changes.

Gamma-aminobutyric acid (GABA) and glycine, the main inhibitory neurotransmitters in the CNS, evoke the characteristic hyperpolarizing responses (IPSPs) in mature neurons only. In immature neurons, however, they elicit depolarizations (e.g., Ben-Ari et al. 1989; Cherubini et al. 1990, 1991; Luhmann and Prince 1991; Wu et al. 1992; Kandler and Friauf 1995; Lo Turco et al. 1995). It has been proposed that this depolarization is important for the maturation of inhibitory neurons by activating voltage-gated Ca^{2+} channels postsynaptically. Ca^{2+} influx mediates cell proliferation and migration, neurite growth, and synaptogenesis (Ben-Ari 2002; Spitzer et al. 2002). Both neurotransmitters activate chloride (Cl^-) channels by binding to $GABA_A$ or glycine receptors, and the polarity of the response is determined by the intracellular free chloride concentration ($[Cl^-]_i$), which changes with age. In immature neurons, the reversal potential for Cl^- (E_{Cl}) is more positive than the resting membrane potential (V_{rest}) due to a high $[Cl^-]_i$, and the transmembrane electrochemical gradient will lead to an efflux of Cl^- upon activation of the ionotropic receptors. In mature neurons, $[Cl^-]_i$ is

low, E_{Cl} is more negative than V_{rest}, and activation of the receptors leads to Cl^- influx and, consequently, to hyperpolarization. This was shown for all areas of the central nervous system analyzed so far (Ben-Ari 2001), e.g., the neocortex (Owens et al. 1996), the hippocampus (Rivera et al. 1999), the brainstem (Singer et al. 1998; Ehrlich et al. 1999; Kakazu et al. 1999) and the spinal cord (Sung et al. 2000; Hübner et al. 2001; Ueno et al. 2002).

A favorable system for investigating the maturation of inhibitory synapses is the superior olivary complex (SOC) in the mammalian auditory brainstem. The SOC consists of several nuclei, the major ones being the lateral superior olive (LSO), the medial superior olive (MSO), the medial nucleus of the trapezoid body (MNTB), and the superior paraolivary nucleus (SPN). The first three are known to be involved in sound localization (reviews: Helfert et al. 1991; Grothe 2000). Adult LSO neurons receive excitatory, glutamatergic input from the ipsilateral ear via the cochlear nucleus and inhibitory, glycinergic input from the contralateral ear via the MNTB. These binaural inputs allow the processing of interaural level differences. During perinatal development (E18–P8), however, glycinergic transmission evokes depolarizing responses in rat and mouse LSO neurons due to a high $[Cl^-]_i$ (Kandler and Friauf 1995; Ehrlich et al. 1999; Kakazu et al. 1999; Kullmann and Kandler 2001).

The regulation of $[Cl^-]_i$ in LSO neurons is affected by loop diuretic drugs (Ehrlich et al. 1999; Kakazu et al. 1999), indicating that cation-coupled chloride cotransporters (CCCs) are involved in this process. These secondary active and electroneutral cotransporters form a gene family that consists of two branches, the Na^+-coupled branch with NCC, NKCC1 and NKCC2, and the K^+-coupled branch with KCC1, KCC2, KCC3 and KCC4 (reviews: Russell 2000; Alvarez-Leefmans 2001; Delpire and Mount 2002). Being driven by the inward-directed Na^+ gradient, the Na^+-coupled cotransporters are capable of transporting Cl^- against its electrochemical gradient into the cells, as seen in immature neurons. In contrast, KCC cotransporters use the outward-directed K^+ gradient to extrude Cl^-, thereby lowering $[Cl^-]_i$, as seen in mature neurons. With the exception of the thiazide-sensitive NCC, all family members are sensitive to loop diuretic drugs such as furosemide and bumetanide (reviews: Aickin 1990; Russell 2000).

Functional analysis of GABAergic neurotransmission in the rat hippocampus revealed that upregulation of *KCC2* expression renders the neurons hyperpolarizing during development, thereby identifying KCC2 as the Cl^- cotransporter in mature hippocampal neurons (Rivera et al. 1999). On the other hand, the most obvious candidate gene for intracellular Cl^- accumulation in immature neurons is *NKCC1*. This is evidenced by in situ hybridization and immunohistochemistry experiments, which demonstrate that both the mRNA and the protein of *NKCC1* are abundant in young hippocampal neurons (Plotkin et al. 1997; Clayton et al. 1998; Marty et al. 2002). However, an expression analysis of *NKCC1* and *KCC2* in the rat brainstem demonstrated that immature LSO neurons (P0–3) do not express *NKCC1* at detectable levels, yet they highly express *KCC2* as do mature LSO neurons (P12) (Balakrishnan et al. 2003). Thus, immature LSO neurons, in contrast to immature hippocampal neurons, appear to generate the high $[Cl^-]_i$ via an inward-directed Cl^- cotransporter other than NKCC1. Moreover, they do not display any upregulation of KCC2 during postnatal maturation. This raises the important question of whether other members of the CCC family are present in the developing LSO and whether $[Cl^-]_i$ regulation in different brain regions may be achieved by different mechanisms. To address these questions, we examined here the expression of five CCC members (*NCC, NKCC2, KCC1, KCC3,* and *KCC4*) during early postnatal development of rats by means of tissue-specific RT-PCR and in situ hybridization. In addition, we analyzed the gene expression of the HCO_3^-/Cl^- exchanger AE3 (Kopito et al. 1989). The AE gene family is composed of three members (*AE1–AE3*) and encodes electroneutral anion exchangers that serve as uphill Cl^- accumulation systems, e.g., in cardiac and smooth muscle cells (Vaughan-Jones 1986; Aickin 1990). Analysis of the anion exchange in red blood cells indicated that the AE family is sensitive to loop diuretic drugs, too (Brazy and Gunn 1976; Gunn 1985). Given these characteristics, AE3 may also be involved in $[Cl^-]_i$ regulation of developing LSO neurons. The observed expression patterns point to AE3 as a candidate for Cl^- loading in immature LSO neurons, resulting in depolarizing glycinergic action. Thermodynamic considerations are presented in support of this presumptive role.

Materials and methods

RNA isolation and RT-PCR

Sprague-Dawley rat pups were anesthesized by a peritoneal injection of 500 mg/kg ketamine and sacrificed by decapitation. The day of birth was defined as P0. All protocols complied with the current German Animal Protection Law and were approved by the local animal care and use committee (Landesuntersuchungsamt Koblenz). Organs were removed and immediately frozen in liquid nitrogen except for brains, which were further dissected under visual inspection. Brainstem tissue was obtained by blocking the brain rostrally to the inferior colliculus and caudally at the medullary level behind the cerebellum. The cerebellum was removed by cutting through the cerebellar pedunculi, and the remaining part of the brain was defined as brainstem. Due to the clear hallmarks, the reproducibility of the preparation is rather high and ensures that the SOC is entirely contained in the tissue sample, whereas the contamination with diencephalic or spinal tissue is minimal. Total RNA was isolated from various rat tissues by the guanidine thiocyanate method and both the quality and quantity of the RNA samples were assessed by gel electrophoresis and optical density measurements. Reverse transcription of total RNA (20 µg) was performed using standard protocols with random hexanucleotide priming and Superscript II reverse transcriptase (Invitrogen) as enzyme in a total volume of 25 µl. After reverse transcription, 175 µl TE buffer (10 mM TRIS-HCl pH 7.4, 1 mM EDTA) was added and 2 µl of the diluted sample used for PCR. Gene-specific PCRs were performed in a total volume of 50 µl using the primers and conditions listed in Table 1. The primers for *NKCC2, KCC1,* and *KCC3* were designed as to amplify all known

Table 1 Oligonucleotides and PCR conditions used for gene-specific expression analysis of six different chloride transporters

Name	Oligonucleotide sequence	Accession number	Product size (bp)	Annealing temperature (°C)
AE3-2808f[a]	5'-TCG GCA TTC CCA TCT CCA TC-3'	NM_017049	502	60
AE3-3309r[a]	5'-ACG ATA GAC AGA CCC ACG AG-3'	NM_017049	–	–
AE3-231f[b]	5'-ACA GCG AGC GCG ACT TTG AG-3'	NM_017049	610	60
AE3-840r[b]	5'-TTC ATG TCG TCC AGA TCG GC-3'	NM_017049	–	–
γ-Actin-109f[a]	5'-CCG TGT TTC CTT CCA TCG TC-3'	X52815	934	60
γ-Actin-1042r[a]	5'-CAG ACT GAG TAC TTG CGT TCA G-3'	X52815	–	–
KCC1-2f[a,b]	5'-TGC CTC ACT TCA CCG TGG TG-3'	U55815	498	60
KCC1-499r[a]	5'-TCA GCA GGG TAC AGC AGC AAC-3'	U55815	–	–
KCC1-2f[a,b]	5'-TGC CTC ACT TCA CCG TGG TG-3'	U55815	478	60
KCC1-479r[b]	5'-CAG ATG AGG ACA ATG AGG AG-3'	U55815	–	–
KCC3-2701f[a]	5'-GTG TGG CGA AAG TGC AGC ATA C-3'	AF108831	641	60
KCC3-3341r[a]	5'-ATG GTG ATC ACT TCA CTG TCC AC-3'	AF108831	–	–
KCC3-71f[b]	5'-CTA AGG TAG AGG ACC CAG AG-3'	AF108831	486	56
KCC3-556r[b]	5'-CCT GAA GAA CTC CAG CTG TG-3'	AF108831	–	–
KCC4-29[a,b]	5'-CTG GAA GAT GGC TGC ACT TG-3'	AW530615	480	60
KCC4-508[a,b]	5'-GAC AGC AAC CCC ATG GTA TC-3'	AW530615	–	–
NCC-2411f[a,b]	5'-GGC ACC ATC TTC CAG TCG GAG-3'	NM_019345	607	56
NCC-3017r[a,b]	5'-TGG CAG TAA AAG GTG AGC AC-3'	NM_019345	–	–
NKCC2-3040f[a,b]	5'-GAG GAA AAA TCA ACC GCA TTG-3'	U10096	382	60
NKCC2-3421r[a,b]	5'-CAC GCC ATG TAC AAC AAA TC-3'	U10096	–	–

[a] Oligonucleotides used for tissue RT-PCR
[b] Oligonucleotides used for the generation of in situ hybridization probes. The number in the oligonucleotide name refers to the position of the most 5'-end nucleotide within the respective cDNA sequence

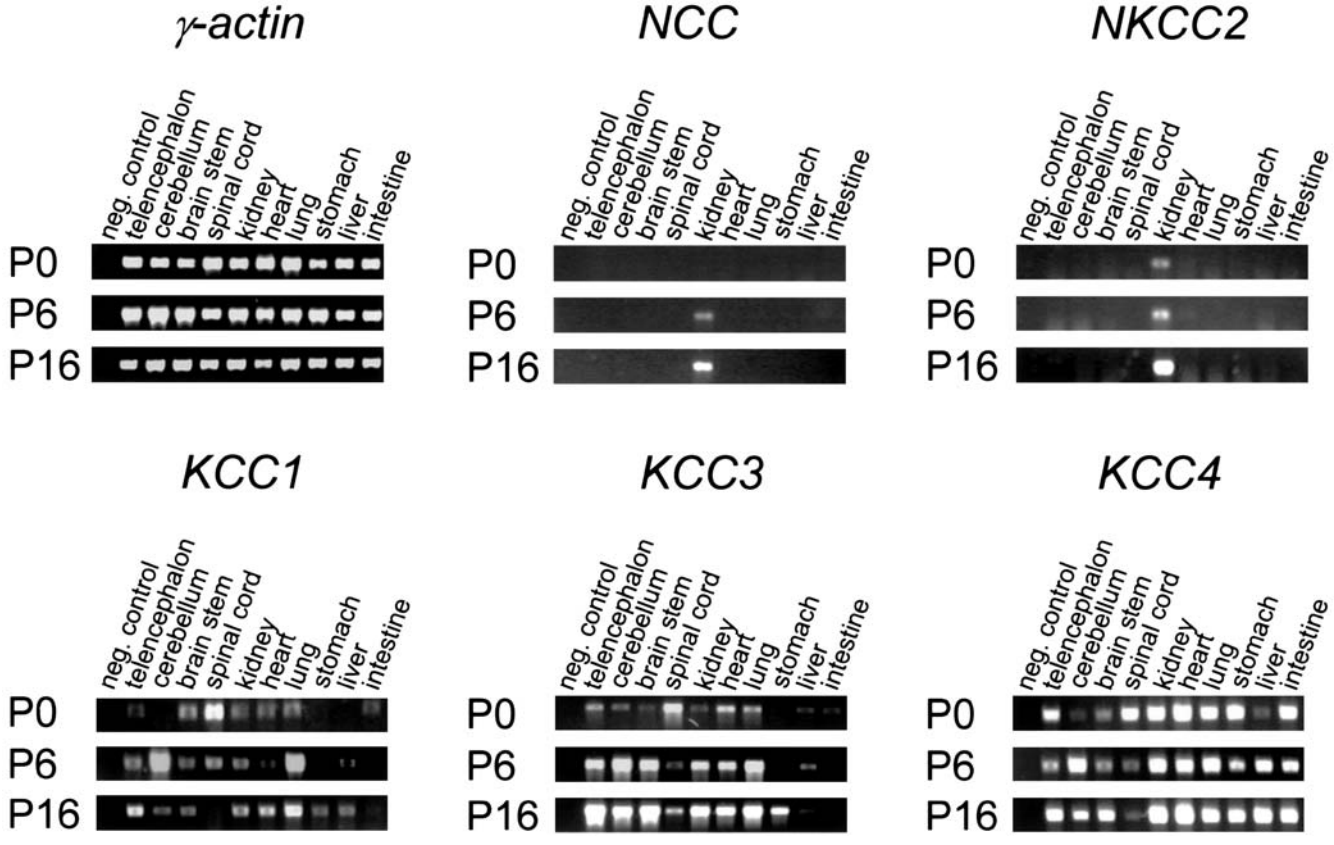

Fig. 1 Expression profiles of five members of the CCC gene family during early postnatal development of rats. Ten tissues and three postnatal ages were investigated for the presence of *NCC, NKCC2, KCC1, KCC3* and *KCC4* by RT-PCR expression analysis. *NCC* and *NKCC2* expression is restricted to the kidney, whereas the three *KCC* members are widely expressed at all three stages. Analysis of *γ-actin* shows a uniform expression in all cDNA pools, indicating equal amounts of cDNA in each RT-PCR reaction. As a negative control, H_2O was added instead of cDNA

splice variants of the respective gene (Table 1) (Payne and Forbush 1994; Hiki et al. 1999; Mount et al. 1999; Race et al. 1999). Generally, denaturing was at 94°C for 30 s, annealing temperature was either 56°C or 60°C for 30 s, and elongation was at 72°C for 1 min. Ten microliters of each reaction were loaded onto a 2% agarose gel containing ethidium bromide (0.5 μg/ml). After electrophoresis, pictures were captured with a CCD camera (768×494 pixels, LTF Labortechnik, Wasserburg, Germany). Each RT-PCR experiment was run twice, based on independent tissue samples, and confirmed the results shown in Fig. 1.

RNA in situ hybridization

Probe synthesis

Gene-specific PCR products (Table 1) were ligated to a T7 promoter using the Lig'n'Scribe PCR promoter addition kit (Ambion), and sense and antisense constructs were obtained by PCR following the manufacturer's instructions. Digoxigenin (DIG)-labeled cRNA probes were generated using the DIG RNA-labeling kit (Roche) and T7 polymerase according to the protocol provided. Probes were analyzed by gel electrophoresis, and approximately 15–30 ng were applied to every section (final concentration 0.5–1 ng/μl). The protocol for DIG-in situ hybridization was modified from Wisden and coworkers (1991).

Histology

Coronal sections of 14 μm thickness, containing the SOC, were cut in a cryostat, thaw mounted on poly-L-lysine-coated slides, and dried for 1.5 h at room temperature. They were fixed in ice-cold 4% paraformaldehyde for 5–15 min. After rinsing in PBS (130 mM NaCl, 7 mM NaH_2PO^4, 3 mM Na_2HPO^4, pH 7.4), sections were transferred for several minutes to 70% ethanol and then stored at 4°C in 100% ethanol until used. Prior to hybridization, sections were permeabilized in 0.1 N HCl for 10 min. After rinsing in PBS, sections were transferred into 0.25% acetic anhydride in 0.1 M triethanolamine, pH 8.0/0.9% NaCl for 10 min, and thereafter into 70% ethanol for 1 min, 95% ethanol for 2 min, 100% ethanol for 1 min, 100% chloroform for 5 min and then back to 100% ethanol and subsequently into 95% ethanol before being air dried. Prehybridization occurred at 50°C in a buffer containing 50% formamide, 4×SSC (600 mM NaCl, 60 mM Na_3 citrate, pH 7.0), 10% dextran sulfate, 5×Denhardt's solution, and 200 mg/ml acid-alkali cleaved salmon sperm DNA. After 2 h, the prehybridization buffer was removed and replaced by the same buffer containing the respective probe. Hybridization was performed overnight at 65°C. Sections were washed for 30 min at 60°C in 4×SSC, 50% formamide, and twice in 1 × SSC. After RNase A treatment (20 μg/ml) for 15 min at 37°C, they were washed twice for 20 min at 50°C in 1×SSC. Bound DIG-labeled probes were detected by using an anti-DIG F_{ab} fragment linked to alkaline phosphatase and 4-nitroblue tetrazolium chloride/5-bromo-4-chloro-3-indolylphosphate as substrate.

Digital images were acquired with a CCD camera system (Hamamatsu C4742–95, 12 bit, 1,280×1,024 pixel, Hamamatsu Photonics, Herrsching, Germany) mounted on a Zeiss bright-field microscope (Axioskop 2, Oberkochen, Germany) and controlled by AnalySIS software (version 3.0, SIS, Münster, Germany). Contrast and brightness were processed using standard image processing software.

Results

Tissue-specific expression of cation-coupled chloride cotransporter genes

To generally assess which of several cation-coupled chloride cotransporter genes (*NCC, NKCC2, KCC1, KCC3*, and *KCC4*) are potential candidates for differential $[Cl^-]_i$ regulation in the maturing auditory brainstem, we first performed RT-PCR experiments on total rat brainstem RNA at P0, P6, and P16. The resulting expression pattern was compared to that obtained from other tissues, i.e., telencephalon, cerebellum, spinal cord, kidney, heart, lung, stomach, liver, and intestine (Fig. 1).

NCC and *NKCC2* expression were confined to the kidney, with *NKCC2* being present at all three ages examined, whereas *NCC* was only expressed at P6 and P16, thus appearing to be upregulated during the first two postnatal weeks (Fig. 1, Table 2). These results are in accordance with previous reports (Gamba et al. 1994; Payne and Forbush 1994). In situ hybridization confirmed the absence of *NCC* and *NKCC2* expression in all four major SOC nuclei (Table 3). *KCC1* expression was detected in most tissues except the cerebellum, stomach, and liver at P0, the stomach and intestine at P6, and the spinal cord and intestine at P16 (Fig. 1, Table 2). *KCC3* also showed a widespread expression pattern. Only in the stomach (P0 and P6) and the intestine (P6 and P16) did we observe no amplification product (Fig. 1, Table 2). Finally, *KCC4* showed a ubiquitous expression pattern during all three stages analyzed, including neuronal tissues (Table 2). In summary, neither of the two inward-directed, Na^+-coupled Cl^- cotransporters *NCC* and *NKCC2* is expressed in the rat brainstem between P0 and P16, whereas all of the outward-directed, K^+-coupled Cl^- cotransporters show expression during that period (Table 2).

Downregulation of *KCC1* expression in developing SOC neurons

As the RT-PCR analysis showed that *KCC1, KCC3,* and *KCC4* are candidate genes for active Cl^- regulation in the brainstem, we next performed RNA in situ experiments with DIG-labeled probes in order to obtain a higher resolution for the localization and abundance of each mRNA in the SOC. These experiments were done at P3 and P12, when glycine depolarizes and hyperpolarizes SOC neurons, respectively. At P3, *KCC1* expression was weak in the LSO, the MSO, and the SPN, whereas the signal intensity was not above background in the MNTB (Fig. 2A) and did not differ from that seen in control sections treated with the sense probe (Fig. 2B). Expression of *KCC1* was also observed in the caudal pontine reticular formation (PnC) and at a similar signal intensity to that observed in the LSO, the MSO, and the SPN (Fig. 2A, B). At P12, no *KCC1* expression was detected, indicating a complete downregulation of this cotrans-

Table 2 Distribution and relative abundance of chloride transporter mRNAs in various rat tissues. Relative expression levels are based on visual inspection of RT-PCR products (n.d. not detected, (+) low expression, + moderate expression, ++ strong expression)

Organ/tissue	Age	NCC	NKCC2	KCC1	KCC3	KCC4	AE3
Telencephalon	P0	n.d.	n.d.	+	++	++	+
	P6	n.d.	n.d.	+	++	++	++
	P16	n.d.	n.d.	++	++	++	++
Cerebellum	P0	n.d.	n.d.	n.d.	+	(+)	+
	P6	n.d.	n.d.	++	++	++	++
	P16	n.d.	n.d.	+	++	++	++
Brainstem	P0	n.d.	n.d.	+	+	+	+
	P6	n.d.	n.d.	+	++	+	++
	P16	n.d.	n.d.	+	++	++	++
Spinal cord	P0	n.d.	n.d.	++	++	++	++
	P6	n.d.	n.d.	+	+	+	+
	P16	n.d.	n.d.	n.d.	+	+	+
Kidney	P0	n.d.	+	+	+	++	+
	P6	+	+	+	++	++	++
	P16	++	++	+	++	++	+
Heart	P0	n.d.	n.d.	+	++	++	++
	P6	n.d.	n.d.	(+)	++	++	++
	P16	n.d.	n.d.	++	++	++	++
Lung	P0	n.d.	n.d.	+	++	++	+
	P6	n.d.	n.d.	++	++	++	++
	P16	n.d.	n.d.	++	++	++	++
Stomach	P0	n.d.	n.d.	n.d.	n.d.	++	+
	P6	n.d.	n.d.	n.d.	n.d.	++	++
	P16	n.d.	n.d.	+	++	++	(+)
Liver	P0	n.d.	n.d.	n.d.	(+)	+	(+)
	P6	n.d.	n.d.	(+)	+	++	n.d.
	P16	n.d.	n.d.	+	(+)	++	(+)
Intestine	P0	n.d.	n.d.	+	(+)	++	(+)
	P6	n.d.	n.d.	n.d.	n.d.	++	+
	P16	n.d.	n.d.	n.d.	n.d.	++	(+)

Table 3 SOC-specific expression data of the chloride transporters. Relative expression levels were estimated by visual comparison of the hybridization signals: n.d. not detected, + moderate, ++ high, LSO lateral superior olive, MNTB medial nucleus of the trapezoid body, MSO medial superior olive, SPN superior paraolivary nucleus

Nucleus	Age	NCC	NKCC1[a]	NKCC2	KCC1	KCC2[a]	KCC3	KCC4	AE3
LSO	P3	n.d.	n.d.	n.d.	+	++	n.d.	n.d.	++
	P12	n.d.	n.d.	n.d.	n.d.	++	n.d.	+	++
MNTB	P3	n.d.	n.d	n.d.	n.d.	++	n.d.	n.d.	++
	P12	n.d.	+	n.d.	n.d.	++	n.d.	+	++
MSO	P3	n.d.	n.d	n.d.	+	++	n.d.	n.d.	++
	P12	n.d.	+	n.d.	n.d.	++	n.d.	+	++
SPN	P3	n.d.	n.d	n.d.	+	++	n.d.	n.d.	++
	P12	n.d.	+	n.d.	n.d.	++	n.d.	+	++

[a] Galakrishnan et al. 2003

porter in the SOC (Fig. 2C, D). Based on these expression data (Table 3), KCC1 most likely plays no role in generating a low $[Cl^-]_i$ in mature LSO neurons.

No expression of *KCC3* in the SOC at P3 and P12

In situ hybridization analysis of *KCC3* in the SOC revealed no detectable expression of this gene at both P3 and P12, as no labeling above background was observed (Fig. 3A–D, Table 3). This rules out KCC3 as a candidate for $[Cl^-]_i$ regulation in LSO neurons during the first two postnatal weeks. The possibility of a non-functional antisense probe can be excluded, because clear signals were obtained in a dot-blot experiment (results not shown).

Weak expression of *KCC4* in the SOC at P12

The analysis of *KCC4* in the SOC revealed no expression at P3 (Fig. 4A, B). At P12, a low level of mRNA was detected (Fig. 4C, D). Neurons in all four major SOC nuclei were clearly labeled above background. This expression was not confined to the SOC, because a signal was also observed in the caudal pontine reticular formation, although at a slightly lower level. Of all three KCC isoforms analyzed, *KCC4* was the only one found to be upregulated during development in the SOC (Table 3).

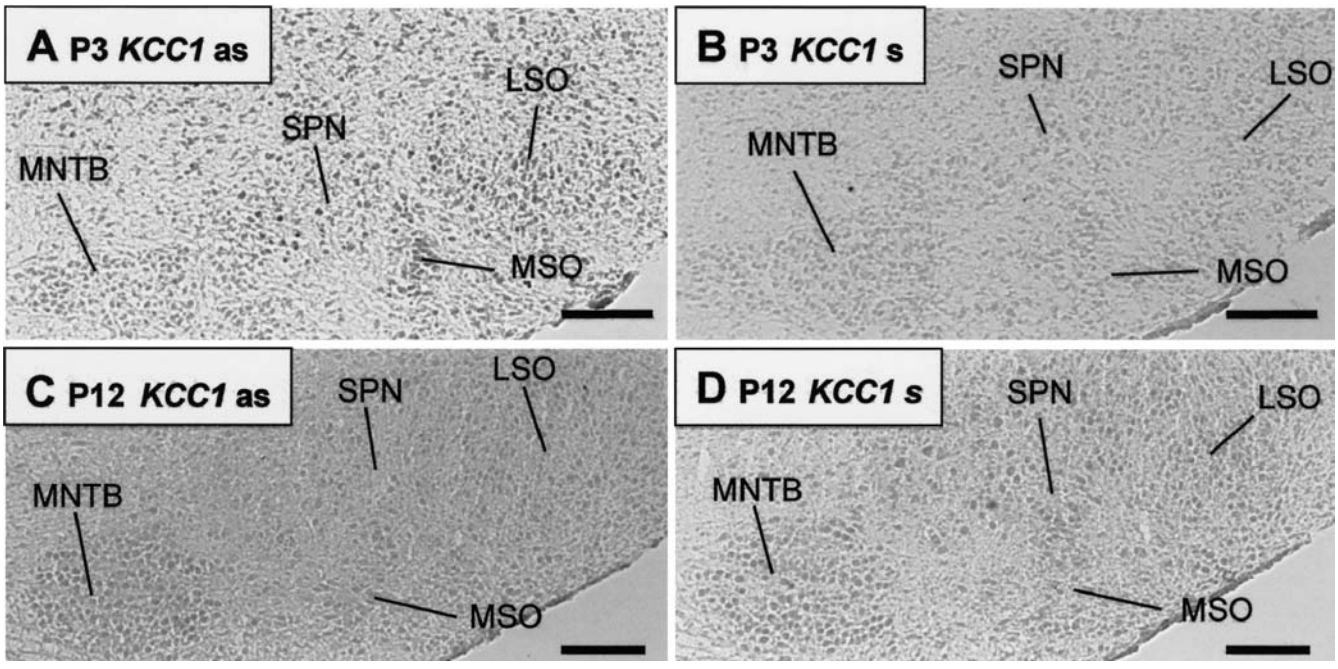

Fig. 2A–D Downregulation of *KCC1* expression in the developing superior olivary complex (SOC) of rats. Coronal sections at P3 and P12 were hybridized with digoxigenin (DIG)-labeled *KCC1* cRNA probes. **A** At P3, weak expression is detected in the lateral superior olive (*LSO*), the medial superior olive (*MSO*), and the superior paraolivary complex (*SPN*), whereas signal intensities in the medial nucleus of the trapezoid body (*MNTB*) are not above background. **B** P3 control section, hybridized with DIG-labeled *KCC1* sense (*s*) cRNA. **C** No *KCC1* expression was detected in the SOC at P12, hybridized with *KCC1* antisense (*as*) cRNA. **D** P12 control section, hybridized with DIG-labeled *KCC1* sense (*s*) cRNA. *Scale bars* 200 μm

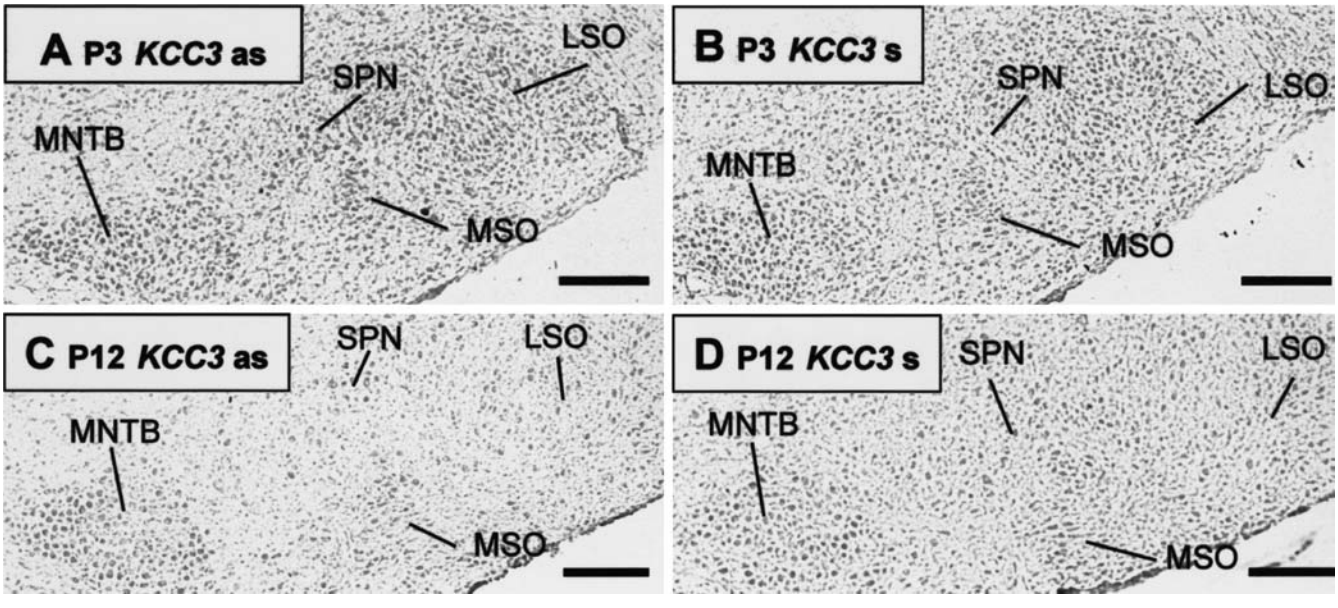

Fig. 3A–D No expression of *KCC3* in the developing rat SOC. Coronal sections at P3 and P12 were hybridized with DIG-labeled *KCC3* cRNA probes. No signal was observed at either stage analyzed. **A** P3 coronal section, hybridized with *KCC3* antisense (*as*) probe. **C** P12 coronal section, hybridized with *KCC3* antisense (*as*) cRNA. **B, D** P3 and P12 control sections, hybridized with *KCC3* sense (*s*) cRNA. *Scale bars* 200 μm

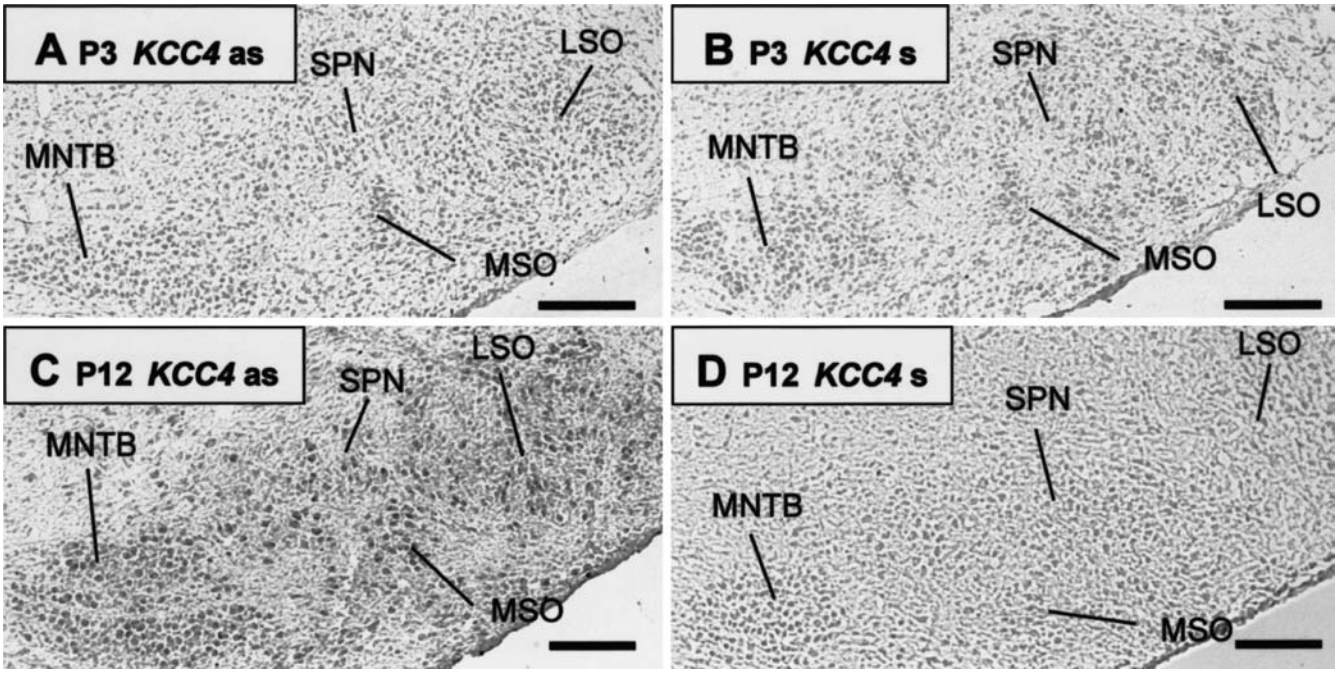

Fig. 4A–D Upregulation of *KCC4* expression in the rat SOC during development. Coronal sections at P3 and P12 were hybridized with DIG-labeled *KCC4* cRNA probes. **A** At P3, no *KCC4* expression was detected in the SOC. **C** All four major nuclei of the SOC show a weak expression of *KCC4* at P12. **B, D** P3 and P12 control sections, hybridized with *KCC4* sense (*s*) cRNA. *Scale bars* 200 μm

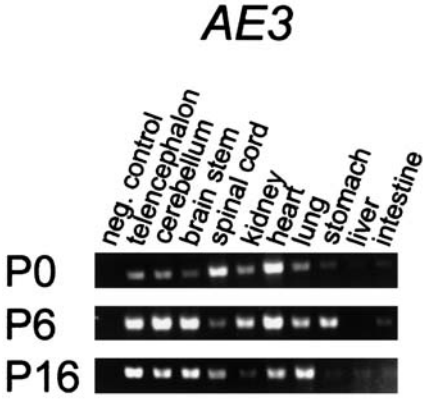

Fig. 5 Widespread expression in several tissues of *AE3* during early postnatal development of rats. RT-PCR analysis of *AE3* expression in ten different tissues at P0, P6, and P16. *AE3* was persistently highly expressed in CNS, heart, and lung as well as in most other tissues, albeit at lower levels

However, the weak labeling indicates a low mRNA abundance and suggests that KCC4 may play only a minor role, if at all, in lowering $[Cl^-]_i$ in mature LSO neurons.

Tissue-specific expression of the HCO_3^-/Cl^- exchanger gene *AE3*

Our results demonstrating an absence of *NKCC* and *NCC* expression in the SOC (Table 3 and Balakrishnan et al. 2003) prompted us to search for alternative candidates being able to actively load LSO neurons with Cl^-. One such candidate is the HCO_3^-/Cl^- exchanger AE3. We first analyzed the expression of this transporter in the developing brainstem by RT-PCR experiments and again compared the pattern with that seen in other tissues. As several splice variants exist, a primer pair was chosen at the 3'-end. This part of the gene seems to be present in most of the *AE3* splice variants as judged by Northern blot and cloning experiments (Kudrycki et al. 1990; Linn et al. 1992). The analysis revealed *AE3* expression in every tissue investigated except the liver (Fig. 5, Table 2). Independent of age, a high expression was observed in the heart and in most brain tissues. Low expression levels were found in the intestines at all ages.

Persistent *AE3* expression in the developing SOC

In situ hybridization experiments of *AE3* revealed a strong expression of the gene in the SOC both at P3 and P12. *AE3* mRNA was detected in the LSO, the MNTB, the MSO, and the SPN with no apparent differences in expression levels both between the nuclei and the developmental stages analyzed (Fig. 6A–D, Table 3). The expression of *AE3* was not confined to the SOC, as

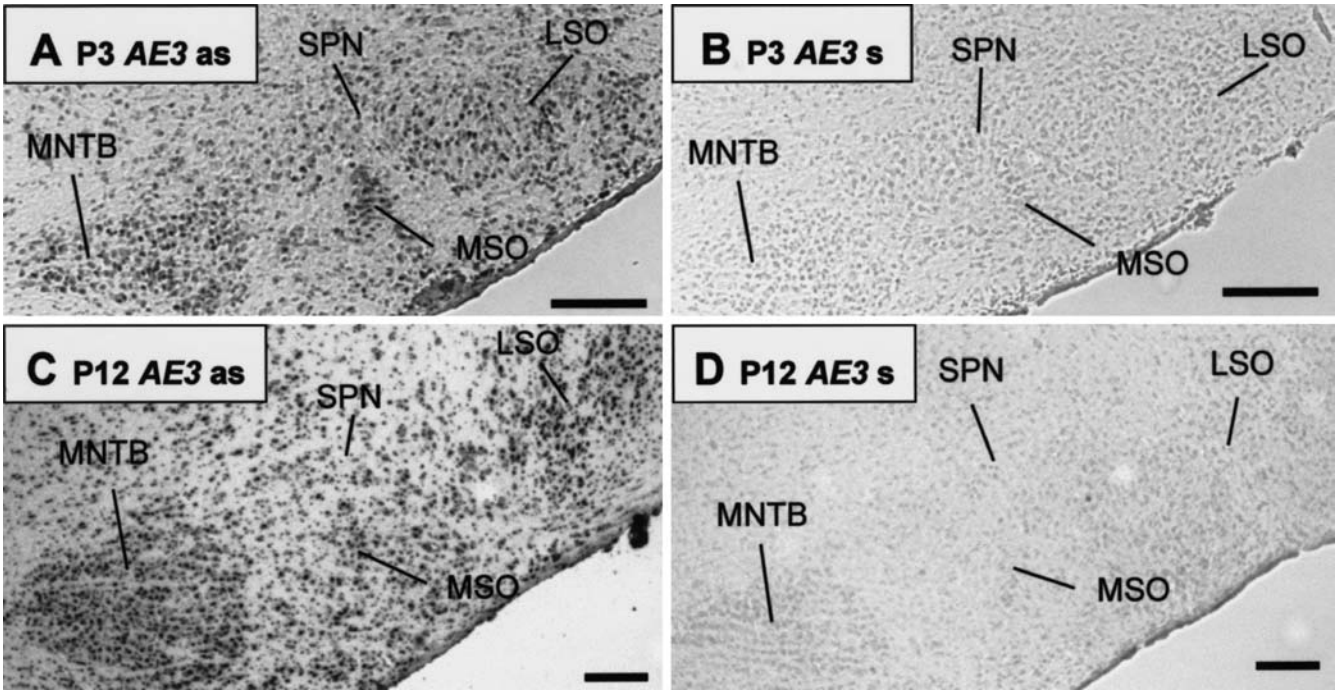

Fig. 6A–D Strong and persistent expression of *AE3* in the developing SOC. Coronal sections at P3 and P12 were hybridized with DIG-labeled *AE3* cRNA probes. **A** At P3, a strong expression was detected throughout the SOC after hybridization with *AE3* antisense (*as*) cRNA. **C** High expression of *AE3* persisted in the SOC at P12, as detected by hybridization with *AE3* antisense (*as*) cRNA. **B, D** P3 and P12 control sections, hybridized with *AE3* sense (s) cRNA. *Scale bars* 200 µm

intense labeling was also observed in the caudal pontine reticular formation (Fig. 6A, C). These results suggest that AE3 may be involved in $[Cl^-]_i$ regulation in the LSO.

Discussion

In this study, we used the techniques of RT-PCR and in situ hybridization to analyze the spatial and temporal expression of six Cl^- transporter genes in the developing rat auditory brainstem. Three of the transporters (NCC, NKCC2, and AE3) are potential candidates for Cl^- intrusion and can therefore be expected to be expressed during early development, whereas the other three (KCC1, KCC3, KCC4) will extrude Cl^- and are likely to be present in mature neurons. Our results show that: (1) most of these six transporters are expressed in the brainstem (RT-PCR) but (2) only *AE3* is predominantly expressed in both immature and mature LSO neurons (in situ hybridization). Together with the results from another study (Balakrishnan et al. 2003), in which we found a high expression of *KCC2* both in neonatal and mature LSO neurons, these data indicate major functions of KCC2 and AE3 in the developing LSO.

Widespread expression of most Cl^- transporters in developing rat tissues

Chloride movements across membranes play an important role in several physiological functions, such as regulation of cell volume and intracellular pH, transepithelial salt absorption or secretion, and modulation of neuronal excitability (review: Alvarez-Leefmans 2001). Consequently, Cl^- is actively transported in virtually all cell types and $[Cl^-]_i$ appears to be tightly regulated. $[Cl^-]_i$ is determined by the combined activity of cotransporters, exchangers, primary active chloride transporters, and chloride channels. The assumption that a variety of transporters contribute to $[Cl^-]_i$ regulation is corroborated by our RT-PCR data, which show that four or more Cl^- transporter types are simultaneously expressed in most tissue types during development (Table 2). To our knowledge, this study, together with a parallel paper (Balakrishnan et al. 2003), forms the first comprehensive expression analysis of Cl^- transporters during early postnatal development of rats. We investigated the six transporters in ten different tissues and applied the sensitive method of RT-PCR, rather than a Northern blot analysis, in order to detect low mRNA levels while globally analyzing a given tissue. A low RT-PCR signal can reflect a generally low gene expression in this tissue. Alternatively, it may imply that the gene expression is limited to a subset of cells. Such a confined expression may be of functional significance, allowing the cellular

differentiation within a tissue or an organ. Furthermore, the PCR technique allows for high-throughput analysis.

Most of our data obtained by the RT-PCR method are in good agreement with previous reports, although the latter mostly analyzed adult tissues. Both Na^+-coupled chloride transporters analyzed (NCC and NKCC2) were previously shown to be kidney specific (Gamba et al. 1993, 1994), and our results are consistent with this finding. *KCC1* and *KCC4* are considered to be "housekeeping" genes (Gillen et al. 1996; Mount et al. 1999) and their widespread expression is confirmed by our RT-PCR results. *KCC3* was reported to display a more restricted expression pattern (Hiki et al. 1999; Mount et al. 1999; Race et al. 1999). Our observation of a widespread *KCC3* expression may be due either to the more sensitive RT-PCR method compared to the reported Northern blot experiments or to the fact that our analysis focused on developing tissues. KCC3 was recently suggested to be involved in cell cycle regulation (Shen et al. 2001), and higher proliferation rates in developing tissues may therefore account for the higher expression levels. Finally, *AE3* was strongly expressed in the brain, the heart, and the lung, and also, yet at lower levels, in other tissues. These data are consistent with reports of its predominant expression in the brain and the heart (Kopito et al. 1989; Kudrycki et al. 1990). Its presence in other tissues, such as the lung, is supported by Northern blot analyses (Kudrycki et al. 1990) and by the presence of *AE3*-derived expressed sequence tags (ESTs) in various libraries of the Washington University-Merck project (Boguski 1995).

Only *AE3* is abundantly expressed in neonatal LSO neurons

Despite their abundant expression in the brainstem demonstrated in our RT-PCR experiments, neither of the three KCC members analyzed (*KCC1, KCC3, KCC4*) is substantially expressed during maturation of LSO neurons. As no or only a low expression was also observed in other regions of the brainstem (data not shown), the signals in the RT-PCR experiments likely reflect a low general expression that was not detected by the less sensitive in situ hybridization technique. *KCC1* and *KCC4* are weakly expressed at P3 and P12, respectively, whereas *KCC3* is not expressed at either age. The only gene showing a high expression level in the SOC, both at P3 and P12, is *AE3*. This suggests an age-independent involvement of AE3 in Cl^- regulation in LSO neurons. In red blood cells, the anion exchanger isoform is sensitive to bumetanide (Brazy and Gunn 1976; Gunn 1985). The amino acid sequence similarity ($\geq$50%) of the various AE family members (Kudrycki et al. 1990) suggests that AE3 is also sensitive to loop diuretic drugs. Such drugs block the Cl^- inward transport in neonatal LSO neurons (Ehrlich et al. 1999), qualifying AE3 as a participant in this process. The high expression level of *AE3* at both ages is also compatible with the well-known role of anion exchangers in intracellular pH regulation (Kopito et al. 1989; Raley-Susman et al. 1993).

Thermodynamic considerations of Cl^- transport

Our expression data obtained at the RNA level point to AE3 as the inward-directed Cl^- transporter in LSO neurons during the depolarizing phase of glycine action. One possible way of addressing the question of whether AE3 may indeed play a significant role in determining $[Cl^-]_i$ in the immature LSO is to compare the values of $[Cl^-]_i$ that this transporter can achieve with those deduced from experimentally determined values of $[Cl^-]_i$. AE3 is an electroneutral cotransporter; consequently, its driving force ($\Delta\mu_{AE}$) is independent of the membrane potential and solely determined by the chemical gradients for the transported ions. It follows that:

$$\Delta\mu_{AE} = RT \ln \frac{\left[HCO_3^-\right]_i}{\left[HCO_3^-\right]_o} + RT \ln \frac{[Cl^-]_o}{[Cl^-]_i}$$

By definition, the system attains equilibrium, i.e., there is no net transport, when $\Delta\mu_{AE}$=0. Under these conditions,

$$RT \ln \frac{\left[HCO_3^-\right]_i}{\left[HCO_3^-\right]_o} = RT \ln \frac{[Cl^-]_i}{[Cl^-]_o}$$

and, hence, $[Cl^-]_i$ calculates to:

$$\frac{\left[HCO_3^-\right]_i \times [Cl^-]_o}{\left[HCO_3^-\right]_o} = [Cl^-]_i$$

In a parallel study (Balakrishnan et al. 2003), gramicidin-perforated patch clamp measurements were performed to determine the glycine reversal potential (E_{Gly}) and to calculate $[Cl^-]_i$ by the Nernst equation (with the understanding that E_{Gly}=E_{Cl}; Ehrlich et al. 1999). During these measurements, the ion concentrations in the bath solution relevant for AE3 were as follows: $[HCO_3^-]_o$=25 mM, and $[Cl^-]_o$=133.5 mM. Values of $[HCO_3^-]_i$ were taken from the literature as 8–15 mM (Klinke and Silbernagl 2001). When these ion concentrations are inserted in the above equation, $[Cl]_i$ calculates to 42–80 mM. The experimentally determined $[Cl]_i$ in P3 LSO neurons (44±22 mM; Balakrishnan et al. 2003) is well within this range. Thus, we conclude that AE3 is indeed in the position to act as the inward-directed Cl^- transporter during the depolarizing phase of glycine. The above equation allows the prediction of $[Cl^-]_i$ if AE3 is the only active Cl^--transporting system and no Cl^- or HCO_3^- diffusion process (e.g., via ligand-gated chloride channels and/or ClC channels) acts as a disturbing factor, enabling AE3 to come to the thermodynamic equilibrium.

Concerning the situation in mature LSO neurons, the experimentally determined value of $[Cl^-]_i$ at P12 is 8±5 mM (Balakrishnan et al. 2003), which is in accordance with the idea that KCC2 is the Cl^--extruding carrier in these cells. The difference between the theoretically and the experimentally obtained values of $[Cl^-]_i$ may be

explained by ongoing background diffusion of Cl^- and/or by some continuous, contravening action of AE3, preventing KCCs from obtaining thermodynamic equilibrium.

Our hypothesis (present paper and Balakrishnan et al. 2003) that $[Cl^-]_i$ regulation in the LSO is accomplished by AE3 and KCC2 is based on the assumption that no further Cl^- transporter is active which is sensitive to loop diuretic drugs. Recently, a novel CCC-interacting protein, CIP1, was identified. CIP1 shares ~25% identity in amino acid sequence with members of the CCC family, but so far no substantial transport activity could be shown (Garon et al. 2000). Database analysis suggests the existence of an additional, so far uncharacterized member of the CCC family (cDNA clone FLJ23188, Genebank accession number AK026841) with ~25–30% identity to CCC family members. Whether this clone encodes a functional Cl^- transporter sensitive to loop diuretic drugs is not known. Nevertheless, preliminary in situ hybridization data indicate no expression in LSO neurons, and no or very weak expression in the brain is supported by an EST database analysis (unpublished data).

A general assumption in mRNA expression studies is the correlation between mRNA and protein level. For Cl^- cotransporters, a good correlation has been consistently found when protein and mRNA level were analyzed in parallel, i.e., for *NKCC1* in the forebrain (Plotkin et al. 1997) and for *KCC2* in the hippocampus, cerebellum (Lu et al. 1999), and brainstem (Balakrishnan et al. 2003). However, to unequivocally correlate the expression of *AE3* and *KCC2* with the functional aspect of active and differential $[Cl^-]_i$ regulation in developing LSO neurons, additional physiological studies have to be performed using gene-specific knockout approaches and/or specific pharmacological inhibition. These studies will contribute to the elucidation of the precise molecular mechanisms by which $[Cl^-]_i$ regulation is accomplished in developing inhibitory projections and to the understanding of basic brain function.

Difference between hippocampus and SOC

This study completes the expression analysis of all known Cl^- transporters that are sensitive to loop diuretic drugs in LSO neurons. Our data imply clear differences in the maturation of GABAergic neurotransmission in the hippocampus, where postsynaptic neurons abundantly express several CCC members during early postnatal and/or adult stages, namely *NKCC1* (Plotkin et al. 1997; Kanaka et al. 2001; Marty et al. 2002), *KCC1* (Kanaka et al. 2001), *KCC2* (Rivera et al. 1999; Kanaka et al. 2001), *KCC3* (Pearson et al. 2001), and *AE3* (Kopito et al. 1989; Raley-Susman et al. 1993). *KCC4* expression has so far not been analyzed in the hippocampus. In addition, Cl^- extrusion in the hippocampus becomes effective by an age-related upregulation of *KCC2* expression (Rivera et al. 1999). In contrast, our data suggest that AE3 expression is the basis of intracellular Cl^- accumulation in young LSO cells, resulting in depolarizing responses upon glycine application, and that the decrease of $[Cl^-]_i$ in mature LSO neurons is achieved by recruiting KCC2 to the plasma membrane (Balakrishnan et al. 2003). If AE3 is still active in mature LSO neurons, it will diminish the effect of chloride extrusion by KCC2. The last surmise needs to be tested in physiological experiments.

Acknowledgements We would like to thank Kornelia Ociepka for expert help with the in situ hybridization and Ulrike Sommerlad for help with the RT-PCR experiments.

References

Aickin CC (1990) Chloride transport across the sarcolemma of vertebrate smooth and skeletal muscle. In: Alvarez-Leefmans FJ, Russell JM (eds) Chloride channels and carriers in nerve, muscle and glial cells. Plenum, New York, pp 209–249

Alvarez-Leefmans FJ (1990) Intracellular Cl^- regulation and synaptic inhibition in vertebrate and invertebrate neurons. In: Alvarez-Leefmans FJ, Russell JM (eds) Chloride channels and carriers in nerve, muscle and glial cells. Plenum, New York, pp 109–158

Alvarez-Leefmans FJ (2001) Intracellular chloride regulation. In: Sperelakis N (ed) Cell physiology sourcebook: a molecular approach. Academic, New York, pp 301–318

Balakrishnan V, Becker M, Löhrke S, Nothwang HG, Güresir E, Friauf E (2003) Expression and function of chloride transporters during development of inhibitory neurotransmission in the auditory brainstem. J Neurosci (in press)

Ben-Ari Y (2001) Developing networks play a similar melody. Trends Neurosci 24:353–360

Ben-Ari Y (2002) Excitatory actions of GABA during development: the nature of the nurture. Nat Rev Neurosci 3:728–739

Ben-Ari Y, Cherubini E, Corradetti R, Galarsa J-L (1989) Giant synaptic potentials in immature rat CA3 hippocampal neurones. J Physiol (Lond) 416:303–325

Boguski MS (1995) The turning point in genome research. Trends Biochem Sci 20:295–296

Brazy PC, Gunn RB (1976) Furosemide inhibition of chloride transport in human red blood cells. J Gen Physiol 68:583–599

Cherubini E, Rovira C, Gaiarsa JL, Corradetti R, Ben-Ari Y (1990) GABA mediated excitation in immature rat CA3 hippocampal neurons. Int J Dev Neurosci 8:481–490

Cherubini E, Gaiarsa JL, Ben-Ari Y (1991) GABA: an excitatory transmitter in early postnatal life. Trends Neurosci 14:515–519

Clayton GH, Owens GC, Wolff JS, Smith RL (1998) Ontogeny of cation-Cl-cotransporter expression in rat neocortex. Brain Res 109:281–292

Delpire E (2000) Cation-chloride cotransporters in neuronal communication. News Physiol Sci 15:309–312

Delpire E, Mount DB (2002) Human and murine phenotypes associated with defects in cation-chloride cotransport. Annu Rev Physiol 64:803–843

Ehrlich I, Löhrke S, Friauf E (1999) Shift from depolarizing to hyperpolarizing glycine action in rat auditory neurons is due to age-dependent Cl^- regulation. J Physiol 520:121–137

Gamba G, Saltzberg SN, Lombardi M, Miyanoshita A, Lytton J, Hediger MA, Brenner BM, Hebert SC (1993) Primary structure and functional expression of a cDNA encoding the thiazide-sensitive, electroneutral sodium-chloride cotransporter. Proc Natl Acad Sci U S A 90:2749–2753

Gamba G, Miyanoshita A, Lombardi M, Lytton J, Lee WS, Hediger MA, Hebert SC (1994) Molecular cloning, primary structure, and characterization of two members of the mammalian electroneutral sodium-(potassium)-chloride cotransporter family expressed in kidney. J Biol Chem 269:17713–17722

Garon L, Rousseau F, Gagnon E, Isenring P (2000) Cloning and functional characterization of a cation-Cl-cotransporter-interacting protein. J Biol Chem 275:32027–32036

Gillen CM, Brill S, Payne JA, Forbush BI (1996) Molecular cloning and functional expression of the K-Cl cotransporter from rabbit, rat and human. A new member of the cation-chloride cotransporter family. J Biol Chem 271:16236–16244

Grothe B (2000) The evolution of temporal processing in the medial superior olive, an auditory brainstem structure. Prog Neurobiol 61:581–610

Gunn RB (1985) Bumetanide inhibition of anion exchange in human red blood cells. Biophys J 47:326a

Helfert RH, Snead CR, Altschuler RA (1991) The ascending auditory pathways. In: Altschuler RA, Bobbin RP, Clopton BM, Hoffman DW (eds) Neurobiology of hearing: the central auditory system. Raven, New York, pp 1–25

Hiki K, D'Andrea RJ, Furze J, Crawford J, Woollatt E, Sutherland GR, Vadas MA, Gamble JR (1999) Cloning, characterization, and chromosomal location of a novel human K^+-Cl^- cotransporter. J Biol Chem 274:10661–10667

Hübner CA, Stein V, Hermans-Borgmeyer I, Meyer T, Ballanyi K, Jentsch TJ (2001) Disruption of KCC2 reveals an essential role of K-Cl cotransport already in early synaptic inhibition. Neuron 30:515–524

Kakazu Y, Akaike N, Komiyama S, Nabekura J (1999) Regulation of intracellular chloride by cotransporters in developing lateral superior olive neurons. J Neurosci 19:2843–2851

Kanaka C, Ohno K, Okabe A, Kuriyama K, Itoh T, Fukuda A, Sato K (2001) The differential expression patterns of messenger RNAs encoding K-Cl cotransporters (KCC1, 2) and Na-K-2Cl cotransporter (NKCC1) in the rat nervous system. Neuroscience 104:933–946

Kandler K, Friauf E (1995) Development of glycinergic and glutamatergic synaptic transmission in the auditory brainstem of perinatal rats. J Neurosci 15:6890–6904

Klinke R, Silbernagl S (2001) Lehrbuch der Physiologie, 3rd edn. Thieme, Stuttgart

Kopito RR, Lee BS, Simmons DM, Lindsey AE, Morgans CW, Schneider K (1989) Regulation of intracellular pH by a neuronal homolog of the erythrocyte anion exchanger. Cell 59:927–937

Kudrycki KE, Newman PR, Shull GE (1990) cDNA cloning and tissue distribution of mRNAs for two proteins that are related to the band 3 Cl^-/HCO_3^- exchanger. J Biol Chem 265:462–471

Kullmann PHM, Kandler K (2001) Glycinergic/GABAergic synapses in the lateral superior olive are excitatory in neonatal C57Bl/6J mice. Brain Res 131:143–147

Legendre P (2001) The glycinergic inhibitory synapse. Cell Mol Life Sci 58:760–793

Linn SC, Kudrycki KE, Shull GE (1992) The predicted translation product of a cardiac AE3 mRNA contains an N terminus distinct from that of the brain AE3 Cl^-/HCO_3^- exchanger. Cloning of a cardiac AE3 cDNA, organization of the AE3 gene, and identification of an alternative transcription initiation site. J Biol Chem 267:7927–7935

Lo Turco JJ, Owens DF, Heath MJS, Davis MBE, Kriegstein AR (1995) GABA and glutamate depolarize cortical progenitor cells and inhibit DNA synthesis. Neuron 15:1287–1298

Lu J, Karadsheh M, Delpire E (1999) Developmental regulation of the neuronal-specific isoform of K-Cl cotransporter KCC2 in postnatal rat brains. J Neurobiol 39:558–568

Luhmann HJ, Prince DA (1991) Postnatal maturation of the GABAergic system in rat neocortex. J Neurophysiol 65:247–263

Marty S, Wehrle R, Alvarez-Leefmans FJ, Gasnier B, Sotelo C (2002) Postnatal maturation of Na^+, K^+, $2Cl^-$ cotransporter expression and inhibitory synaptogenesis in the rat hippocampus: an immunocytochemical analysis. Eur J Neurosci 15:233–245

Mehta AK, Ticku MK (1999) An update on GABA(A) receptors. Brain Res Rev 29:196–217

Mount DB, Mercado A, Song LY, Xu J, George AL, Delpire E, Gamba G (1999) Cloning and characterization of KCC3 and KCC4, new members of the cation-chloride cotransporter gene family. J Biol Chem 274:16355–16362

Owens DF, Boyce LH, Davis MB, Kriegstein AR (1996) Excitatory GABA responses in embryonic and neonatal cortical slices demonstrated by gramicidin perforated-patch recordings and calcium imaging. J Neurosci 16:6414–6423

Payne JA, Forbush B III (1994) Alternatively spliced isoforms of the putative renal Na-K-Cl cotransporter are differentially distributed within the rabbit kidney. Proc Natl Acad Sci U S A 91:4544–4548

Pearson MM, Lu J, Mount DB, Delpire E (2001) Localization of the K(+)-Cl(−) cotransporter, KCC3, in the central and peripheral nervous systems: expression in the choroid plexus, large neurons and white matter tracts. Neuroscience 103:481–491

Plotkin MD, Snyder EY, Hebert SC, Delpire E (1997) Expression of the Na-K-2Cl cotransporter is developmentally regulated in postnatal rat brains: a possible mechanism underlying GABA's excitatory role in immature brain. J Neurobiol 33:781–795

Race JE, Makhlouf FN, Logue PJ, Wilson FH, Dunham PB, Holtzman EJ (1999) Molecular cloning and functional characterization of KCC3, a new K-Cl cotransporter. Am J Physiol-Cell Physiol 277:C1210–C1219

Raley-Susman KM, Sapolsky RM, Kopito RR (1993) Cl^-/HCO_3^- exchange function differs in adult and fetal rat hippocampal neurons. Brain Res 614:308–314

Rivera C, Voipio J, Payne JA, Ruusuvuori E, Lahtinen H, Lamsa K, Pirvola U, Saarma M, Kaila K (1999) The K^+/Cl^- co-transporter KCC2 renders GABA hyperpolarizing during neuronal maturation. Nature 397:251–255

Russell JM (2000) Sodium-potassium-chloride cotransport. Physiol Rev 80:211–276

Shen MR, Chou CY, Hsu KF, Liu HS, Dunham PB, Holtzman EJ, Ellory JC (2001) The KCl cotransporter isoform KCC3 can play an important role in cell growth regulation. Proc Natl Acad Sci U S A 98:14714–14719

Singer JH, Talley EM, Bayliss DA, Berger AJ (1998) Development of glycinergic synaptic transmission to rat brain stem motoneurons. J Neurophysiol 80:2608–2620

Spitzer NC, Kingston PA, Manning TJ Jr, Conklin MW (2002) Outside and in: development of neuronal excitability. Curr Opin Neurobiol 12:315–323

Sung KW, Kirby M, McDonald MP, Lovinger DM, Delpire E (2000) Abnormal GABAA receptor-mediated currents in dorsal root ganglion neurons isolated from Na-K-2Cl cotransporter null mice. J Neurosci 20:7531–7538

Ueno T, Okabe A, Akaike N, Fukuda A, Nabekura J (2002) Diversity of neuron-specific K^+-Cl^- cotransporter expression and inhibitory postsynaptic potential depression in rat motoneurons. J Biol Chem 277:4945–4950

Vaughan-Jones RD (1986) An investigation of chloride-bicarbonate exchange in the sheep cardiac Purkinje fibre. J Physiol (Lond) 379:377–406

Wisden W, Morris BJ, Hunt SP (1991) In situ hybridization with synthetic DNA probes. In: Chad J, Wheal H (eds) Molecular neurobiology—a practical approach. IRL, Oxford, pp 205–225

Wu WI, Ziskind-Conhaim L, Sweet MA (1992) Early development of glycine- and GABA-mediated synapses in rat spinal cord. J Neurosci 12:3935–3945